2016 IEEE International Conference on Robotics and Automation (ICRA)
Stockholm, Sweden, May 16-21, 2016

Robot locomotion on hard and soft ground: measuring stability and ground properties in-situ

Will Bosworth[1], Jonas Whitney[2], Sangbae Kim[1], and Neville Hogan[1,3]

Abstract— **Dynamic behavior of legged robots is strongly affected by ground impedance. Empirical observation of robot hardware is needed because ground impedance and foot-ground interaction is challenging to predict in simulation. This paper presents experimental data of the MIT Super Mini Cheetah robot hopping on hard and soft ground. We show that controllers tuned for each surface perform better for each specific surface type, assessing performance using measurements of 1.) stability of the robot in response to self-disturbances applied by the robot onto itself and 2.) the peak accelerations of the robot that occur during ground impact, which should be minimized to reduce mechanical stress. To aid in controller selection on different ground types, we show that the robot can measure ground stiffness and friction in-situ by measuring its own interaction with the ground. To motivate future work in variable-terrain control and in-situ ground measurement, we show preliminary results of running gaits that transition between hard and soft ground.**

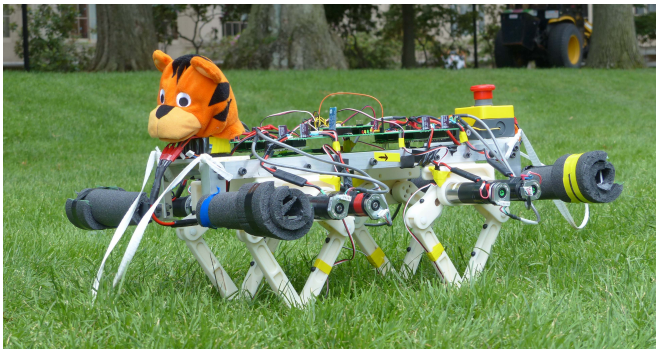

Fig. 1: The Super Mini Cheetah (SMC) quadrupedal robot: a small quadrupedal robot capable of indoor and outdoor behaviors such as walking, hopping, running, turning and stopping. The robot is used in this study to evaluate hopping over hard and soft ground and to measure ground properties in-situ.

I. Introduction

Legged robots are most valuable when they can operate dynamically in unexplored, variable terrain. Foot-ground interaction has a large effect on dynamic locomotion behavior but accurately modeling ground properties and foot-ground interaction a priori is challenging because terrain is highly variable and impact mechanics are complex. For example, ground impedance and surface friction varies significantly between terrain types such as concrete, grass, sand, or mud. Empirical study of dynamic legged robots over many ground types is important to increase robot capability over new ground surfaces and to bridge the gap between simulation and robot hardware.

This paper presents experimental data of hopping on hard and soft ground using the MIT Super Mini Cheetah (SMC) robot, Fig. 1 [1]. To characterize hopping performance, the robot applies self-disturbances through its own legs which create repeatable disturbance responses. Two parameterizations of a hopping controller are examined: one was tuned for hard ground and one was tuned for soft ground. Each controller is shown to be more suitable for its own ground surface. These results show that ground impedance is an important factor in legged locomotion control. We also demonstrate how the robot can measure ground impedance and friction in-situ by interacting with the ground. This perception enables a robot to modify its controller in response to changes in ground type. Finally, we show preliminary results of the SMC robot running between hard and soft ground surfaces. This final experiment motivates ongoing future work to develop controllers for variable terrain and develop methods for in-situ ground property measurement.

Corresponding author bosworth@mit.edu
[1]Author is with the Department of Mechanical Engineering, Massachusetts Institute of Technology, Cambridge, MA 02139.
[2]The Department of Electrical Engineering and Computer Science, MIT.
[3]The Department of Brain and Cognitive Science, MIT.

A. Related work

This study draws on previous work in robot limb design, locomotion planning and control, locomotion over variable terrain, stability measurement of locomotion, and terrain measurement with real robot hardware.

The SMC robot is a new inexpensive and lightweight quadrupedal robot that is capable of running and jumping over many terrain types. The design was motivated by the MIT Cheetah robot which draws inspiration from robot limbs for human-touch interaction such as the Phantom haptic interface arm [2][3]. In this design paradigm, the robot limb is made of lightweight rigid links and powered by backdrivable motors. In contrast, many robot limbs that use actuators with higher intrinsic impedance, such as highly geared electric motors or hydraulic actuators, include elastic elements in the limb to shape the mechanical response of the leg to impacts with the ground [4-12]. Elastic elements can provide robustness and weight-reduction advantages. Alternatively, low-inertia, rigid limbs reduce the complexity of controlling foot force, allow for proprioceptive sensing of contact through the motor port ([13]) and allow for a wide range of limb impedances to be accessed using feedback control, without modification of mechanical hardware. This range of accessible impedances is useful in present-day research, where the best choice of limb impedance remains open research.

The control system in this study uses the SMC robot's ability to control both ground forces and impedance of the leg. It has long been known that tuned leg impedance can provide passive stabilization to locomotion controllers [12]. Modern robots still use tuned limb impedance to achieve efficient locomotion [6] and a class of simulation-based quadrupeds have used parameter search to find impressive running and turning gaits [14][15]. Alternatively, modern trajectory planners are quickly maturing and have yielded impressive locomotion behaviors in simulation [16][17]. These planners find the desired dynamics of a simple reduced model—often a single rigid body [18]—which guides the search of individual joint torque trajectories. Stabilizing force trajectories during cyclic locomotion, particularly in hardware, is an open research topic. Many modern robots have succeeded in stabilizing open-loop trajectories with the addition of leg-level impedance controllers or body-level virtual model controllers ([19]) around open-loop trajectories [2][20][21]; the controller presented in this paper uses both joint and body-level impedance control. The best abstractions between open-loop trajectory planning and feedback control are open design problems in the field, and the development and characterization of new behaviors is necessary for further refinement.

Few studies of robot legged locomotion have quantified performance over varying terrain. Some robots have demonstrated impressive dynamic locomotion outdoors [22-26], though the precise conditions of these outdoor tests are unclear. Other robots have demonstrated variable-height terrain traversal in laboratory settings [20][21][6][9]. The DARPA Robotics Challenge and Learning Locomotion programs resulted in non-ballistic locomotion demonstrations on non-flat terrain [27][28].

To date, there is no consensus on how to assess the stability properties of locomotion on robotic or biological hardware. Some studies compare controller stability by measuring the success rate of different controllers performed over multiple trials [29]. Assessing orbital stability with Floquet multipliers has been performed on human walking, though theoretical analysis suggests that hundreds or thousands of consecutive steps must be performed to overcome the stochasticity of biological walking [30]. A mean time to failure metric of locomotion during random disturbances has been proposed and used in simulation [31]. A recent study presented a comparison of stability metrics on a single hardware platform that operated in variable terrain [32]. That study showed that measures of the leg state and the decay-rate of the body two strides following a step disturbance were good practical predictors of a robot's rough terrain performance.

Measuring ground properties in-situ by observing locomotion performance and foot-ground interaction has been considered for over two decades [33]. Previous legged robots have performed classification of ground types by observing body motion, leg motion, leg torques or foot forces. These experiments have been performed with single robot legs [34], hexapedal walking robots [35] and hexapedal running robots [36][37]. To the best of our knowledge, no legged robot has directly measured ground stiffness or surface friction in-situ. Compared to robots used in previous terrain identification studies, unique features of the SMC robot enable direct ground measurements: each leg can control both vertical and horizontal foot forces during ground interaction and accurately measure resulting foot motion.

The contribution of this paper is to show experimental results of dynamic hopping over both hard and soft ground to highlight the effect that ground impedance has on the stability of a robot that uses modern locomotion control techniques. Given the importance of ground impedance on stability, the paper further demonstrates how a legged robot with adequate control authority can measure ground surface properties such as impedance and friction in real time. The paper proceeds as follows:

- Section II describes the Super Mini Cheetah robot and the controller used in this study.
- Section III presents the performance of two hopping controllers on soft and hard ground.
- Section IV presents the techniques to measure ground friction and surface stiffness.
- Section V presents discussion and future work, including running over transitions from hard to soft ground.
- Section VI presents conclusions of the study.

II. The Super Mini Cheetah robot and control system

This section describes relevant details of the SMC robot; [1] contains an overview of the electromechanical design of the robot.

A. The Super Mini Cheetah robot

The SMC robot was intended for experimentation and replicability: it is lightweight (9 kg), inexpensive ($7k in parts), robust, dynamic, and uses commercial-off-the-shelf components and increasingly common rapid prototyping methods such as 3d printing. The robot's limbs can control force and a wide range of impedances at the foot, which enables it to implement a variety of modern control algorithms. The robot has enough torque density to perform dynamic running and jumping and has proven robust in hundreds of hours of experimentation. The robot's small size makes it possible for a single scientist to transport the robot and perform experiments in the lab or outdoors, and the robot has been shipped on an airplane as regular baggage. Please see the accompanying video for an overview of some behaviors the SMC robot has performed indoors and outdoors.

The leg is the fundamental module of the SMC robot. The leg consists of a five-bar linkage of 3d-printed plastic links connected to two motors in the hip which each contain a 20:1 gearhead. Thus, each leg can actuate in the vertical and horizontal (forward) plane. Open-loop foot force commands are generated using the Jacobian of the leg to calculate required motor torques; torque commands are delivered to high-bandwidth current controllers that drive each motor. As described in [1], the robot leg can generate accurate vertical and horizontal force commands through impact, though a

lightly-damped approximately 30 Hz resonance is present when interacting with stiff surfaces. The intrinsic damping and inertia at the foot are approximately 13 Ns/m and 2 kg, and the leg is capable of generating stiffness and damping values up to 4 kN/m and 4 kNs/m in the vertical direction using feedback control through the motors. The leg has a maximum length of 20 cm and minimum length of 10 cm. Its maximum rotation of the foot about the hip joint is +/- 55°. The position and velocity of each leg is measured using encoders attached to each motor. Each foot has a contact sensor made of a pressure sensor embedded into soft rubber—a design motivated by [38]—and an IMU is attached to the body of the robot[1].

B. Hopping control system

The hopping controller uses event-based state machines which operate on each leg. Each state machine cycles sequentially between a flight state and a stance state. The transition from the flight to stance state is triggered by measuring impact with the ground using a contact sensor on the foot. The transition from the stance to flight state occurs a fixed duration of time after entering the stance state. Each limb is controlled by an independent state machine but the front limbs and rear limbs are often coupled to each other. For example, if a foot sensor on one of the front limbs measures ground contact, both front limbs will enter their stance state.

The stance state consists of open-loop vertical and horizontal force trajectories, joint-level impedance commands and force commands from a body-level virtual model control. Each feedforward force trajectory is a parameterized triangle wave with a duration and peak amplitude. The joint-level impedance controls the stiffness and damping of each motor joint.

During stance, a virtual model controller commands foot forces in response to roll and yaw angles measured by the body. To control body roll, vertical force commands are applied in proportion to error in the roll angle of the robot. To control yaw, horizontal force commands are applied in proportion to the error in yaw angle of the body. This command is applied differentially: to turn to the right, legs on the left side of the robot push forward and legs on the right push backwards. The horizontal force command from the yaw control is limited in magnitude to 20 N. In practice, the SMC robot can control straight-line heading, and perform reliable turning gaits up to $\pi/3$ rad/s on hard, flat ground.

The selection of parameters for the force trajectories, joint impedance commands and virtual model control impedances were guided by offline dynamic simulation and empirical observation on the robot. The force trajectories and joint impedances were guided by a simulation of a planar mass with massless legs that were treated as ideal force sources. A greedy evolutionary search was used to select force trajectory parameters that operated within the force and motion constraints of the real leg. Joint-level impedance was selected by using parameter sweeps of the stiffness and damping gains on the planar model and selecting values that balanced the trade-off between passive stability and accurate tracking of the open-loop force trajectory plan; this resembles the method employed by [2] and corroborates observations from [29]. The virtual model control gains were selected with the aid of a dynamic simulation of the robot built using Open Dynamics Engine and also guided by empirical observation.

[1]The IMU is a Vectornav VN-100 Rugged. A part list for the SMC robot is included in [1].

TABLE I: Control parameters of the hard and soft-ground hopping controllers

Parameter name	State	Hard-ground controller	Soft-ground controller	Unit
Duration	stance	150	200	ms
Peak vert cmd	stance	120	100	N
Horizontal cmd	stance	0	0	N
Joint stiffness[3]	stance	0.2	0.2	Nm/rad
Joint damping	stance	0.01	0.01	Nms/rad
Roll stiffness[4]	stance	100	100	Nm/rad
Yaw stiffness[4]	stance	8	8	Nm/rad
Joint stiffness	flight	0.3	0.45	Nm/rad
Joint damping	flight	0.02	0.05	Nms/rad

III. Hopping on hard and soft ground

This section describes hopping experiments that were performed on hard and soft ground surfaces. The hard surface was a tile floor and the soft surface was a 7.5 cm thick memory foam pad. The stiffness of the memory foam was measured[2] as approximately 10 kN/m.

We report on two parameterizations of the hopping controller described in Sec. II-B – a "hard-ground" controller and a "soft-ground" controller. The hard-ground controller was developed for use on tile floor and parameters were hand-tuned using observations on the tile floor. In initial experiments, this controller performed poorly on soft ground, so a second gait was hand-tuned using observation of the robot on soft foam. This second controller is referred to as the soft-ground controller. The control parameters for the two gaits are described in Table I. The soft-ground controller had a longer stance duration with smaller peak magnitude than the hard-ground controller, as well as larger commanded limb impedance during the flight phase. Larger impedance during the flight phase results in more aggressive swing-leg action which extends to larger dynamic response of the leg at the instant of foot-ground impact.

[2]See Sec. IV-A for methods used to measure ground stiffness.

[3]In Table I, the joint-level impedance values are reported in units at the motor joint. But, these joint-level impedances result in an effective stiffness and damping of the leg as viewed from the foot, which can be calculated using the leg Jacobian. During stance, the vertical stiffness & damping at the foot with respect to the body is approximately 750 [N/m] and 38 [Nm/s].

[4] The "roll stiffness" and "yaw stiffness" in Table I are virtual model gains; see Sec. II-B.

A. Measuring stability from self-disturbance

When observing the gaits in real time, the hard-ground and soft-ground controllers appeared to have qualitatively similar stability properties over hard ground, though the hard-ground controller performed significantly worse on the soft foam surface. Self-disturbance experiments were performed to measure the relative stability of the hopping gaits. In this experiment, the robot performed regular hopping and applied a disturbance force trajectory during one stride. Motion of the robot body throughout the disturbance response was measured using an IMU mounted in the torso of the robot.

Disturbance response data is shown in Fig. 2 for both the hard-ground and soft-ground controllers operating on hard and soft ground. Each trial consisted of 12 seconds of hopping, with the self-disturbance forces applied during the first stance event after three seconds of hopping. The disturbance was applied by adding force to both legs on the left side of the robot. The disturbance was applied by increasing the peak magnitude of the triangle-wave force trajectory (see Sec. II-B). Noting that the duration of the stance state differs for the two controllers, the triangle wave was modified so that the net impulse of the disturbance was equal. The net disturbance impulse was 10 Ns.

The disturbance response results in Fig. 2 contain data from ten trials of each controller. Each plot shows the average and standard deviation of the roll angle of the body. Roll angle was selected because it was the most common failure mode and contained a clear disturbance response. The data were acquired at 250 Hz.

The results show that the disturbance event is identifiable, and that the disturbance responses were repeatable. Each controller-surface combination showed a unique disturbance response. When operating on hard ground (Fig. 2a, 2c), both controllers settled in less than two seconds, though the soft-ground controller showed less total deflection and faster return to the nominal roll angle cycle. The slowest disturbance response occurred with the hard-ground controller on soft ground (Fig. 2b): the response oscillated for nearly seven seconds around the nominal operating point; the larger values of standard deviation show that this controller was the least repeatable. The soft-ground controller showed improved disturbance response on soft ground (Fig. 2d), though the response was still slower than the controllers on hard ground. Videos of some disturbance response trials are included in the video attachment.

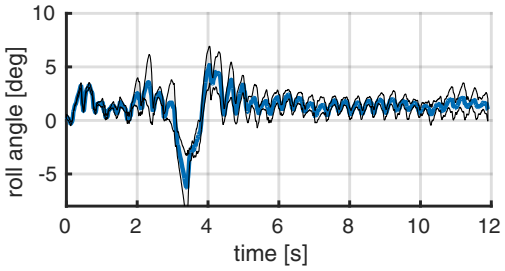

(a) Hard-ground controller hopping on hard ground.

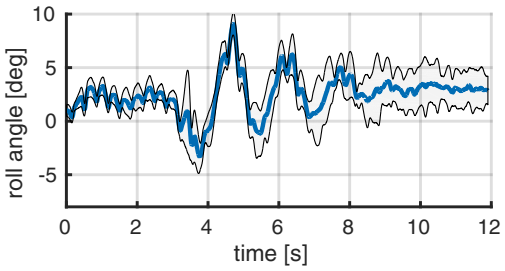

(b) Hard-ground controller on soft ground

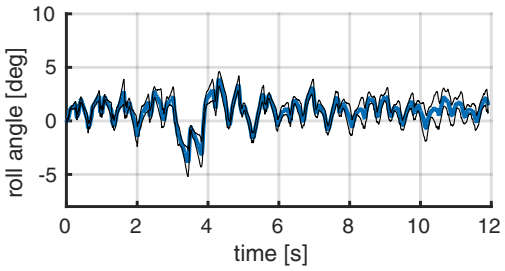

(c) Soft-ground controller on hard ground

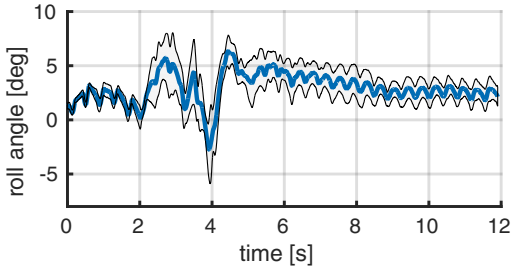

(d) Soft-ground controller on soft ground

Fig. 2: Results of disturbance response trials using two controllers—a hard-ground and soft-ground controller—operating on hard tile and soft foam. Each plot shows the roll angle of the robot over a 12 second window; a disturbance was applied during the third second of each trial. Mean and standard deviation from 10 trials is shown. The disturbance was applied as an additional force command applied by legs on the left side of the robot in order to induce a change in the roll angle. The response of the robot to a disturbance event is clearly visible in each figure. Both controllers exhibited faster settling when operating on hard ground; the soft-ground controller settled faster over both ground types, and the hard-ground controller exhibited the slowest, least repeatable disturbance response.

B. Vertical acceleration during hopping

Although the soft-ground controller demonstrated good disturbance response when operating on hard ground, we prefer to run the hard-ground controller during testing and demonstrations because the soft-ground controller appears to impact the ground harshly—i.e., it is visually and audibly jarring to operate.

Fig. 3 shows vertical acceleration of the body during the hopping experiments on hard ground. The data shows individual plots from all ten trials of the hard-ground and soft-ground control tests. The data in Fig. 3 occurred during a two second window that includes the beginning of the disturbance response shown in Fig. 2. Individual trial results highlight the difference in peak vertical acceleration measured in the body. During each stride, the peak acceleration of the soft-ground controller was nearly 50% larger than the

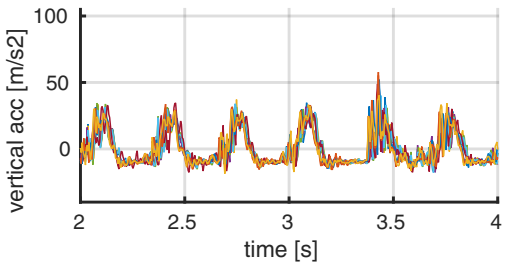

(a) Hard-ground controller on hard ground

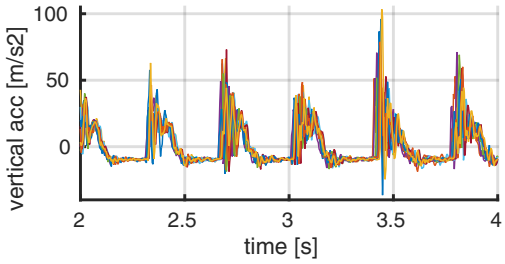

(b) Soft-ground controller on hard ground

Fig. 3: Vertical acceleration of the body of the SMC robot, measured during the disturbance response trials shown in Fig. 2. The hard-ground (a) and soft-ground (b) controllers are shown operating on hard ground which demonstrates that the soft-ground controller resulted in increased peak vertical acceleration of nearly 50% each stride. These results show that the soft-ground controller increased mechanical stress on the robot when operating over hard ground.

hard-ground controller. These results corroborate our initial observation that the soft-ground controller resulted in large peak magnitudes when operating on hard ground, which supports the conclusion that the hard-ground controller is better for operation on hard ground and the soft-ground controller is better for operation on soft ground.

IV. Measuring Ground Properties

The previous section demonstrated that different controllers are better suited for different ground surfaces. To select controllers as terrain varies, a legged robot must also be able to perceive ground surface properties in-situ. This section presents algorithms used by the SMC robot to measure ground properties using direct interaction with the ground. Three results are presented: A.) measuring ground stiffness during standing, B.) characterizing ground type by measuring the acceleration of the body after impact, and C.) measuring the coefficient of static friction between the foot and the ground.

A. Measuring ground stiffness during standing

Ground stiffness can be measured by the SMC robot during standing by the following method: the robot begins standing on a diagonal pair of legs—i.e., the front-left and rear-right legs. A command is sent to instantly shift the weight of the machine from one pair of legs to the other. As the weight of the machine shifts between the leg pairs, the feet move with respect to the body—i.e., the legs that previously supported the weight of the robot retract towards the body while the legs that take the weight of the robot extend into the ground. More compliant ground surfaces result in more deflection of the legs. Using visual inspection and IMU measurements, we verified that the body of the robot does not move significantly compared to the legs. Therefore, measured displacement of the legs is the result of motion at the foot.

During each trial, the change in angle of the leg-motor joints are measured and the resulting displacement of the leg, ΔY, is calculated using the Jacobian of the leg. The vertical stiffness of the leg-ground interface, K_{lg}, is calculated with a linear Hooke's law relationship using leg displacement and robot weight W:

$$K_{lg} = \frac{W}{2\,\Delta Y}. \tag{1}$$

The factor of 1/2 in Eq. 1 accounts for the weight being carried by two legs.

Each leg of the SMC robot contains a rubber contact sensor placed at the foot. The stiffness of the rubber footpad, K_f, was measured as approximately 20 kN/m. This stiffness value is within an order of magnitude of many ground types. Thus, the leg-ground stiffness (Eq. 1) is modeled as two compliant elements in series – the footpad stiffness K_f and the ground stiffness K_g:

$$\frac{1}{K_{lg}} = \frac{1}{K_g} + \frac{1}{K_f} \tag{2}$$

Fig. 4 shows stiffness of the ground, K_g, measured from data acquired during trials of the standing experiment, performed over many surface types. The results show that many surfaces can be distinguished and categorized over more than an order of magnitude of stiffness: foam, rubber, foam core (poster board), damp grass, mulch, and concrete result in repeatably different stiffness measurements. As ground stiffness exceeds footpad stiffness, the dominant source of leg displacement occurs in the footpad, which limits the resolution of stiffness measurement as ground becomes hard—e.g., tile or concrete.

The ground stiffness values measured by the SMC robot were corroborated using lab-bench measurements with a weight scale and video analysis. Stiffness was measured by manually pushing a plastic leg link into ground surface materials and measuring the force and resulting displacement. Ground stiffness is typically not linear, so the measurements were performed near 45 N, the approximate loading in each leg during the standing-experiment. Table II compares stiffness values measured by the SMC robot, from Fig. 4, and stiffness values from direct measurement. The results show that the robot's measurement is consistently lower in magnitude, but both methods result in similar trends over an order of magnitude of stiffness values.

B. Differentiating ground type by impedance during jumping

Fig. 5 shows vertical acceleration of the body during jumping and landing on different ground surfaces. The experimental data shows the vertical acceleration of the body

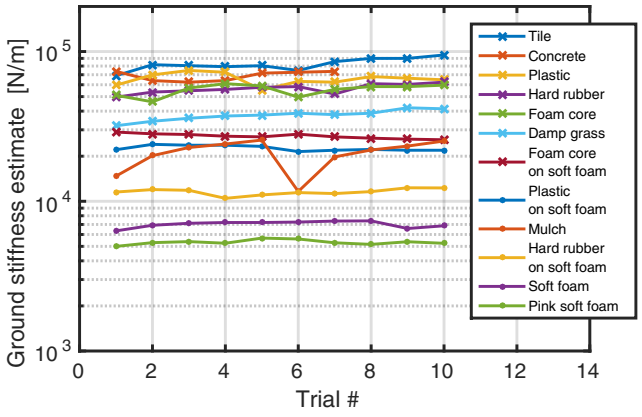

Fig. 4: Stiffness of different ground types measured in-situ by the SMC robot during standing. In this experiment, the robot shifts its weight between pairs of legs while maintaining a static body posture. As legs take on the weight of the robot, the legs extend into the ground. This kinematic data is measured and stiffness is calculated using the assumptions described in Eq. 1 & Eq. 2.
In-situ measurement was carried out over numerous ground surfaces types and repeated up to 10 times for each surface. Note that the "mulch" trial has significant variation; mulch is a non-uniform material that includes soft dirt and bark, so variation in measurements as the robot is moved through a mulch surface is plausible.

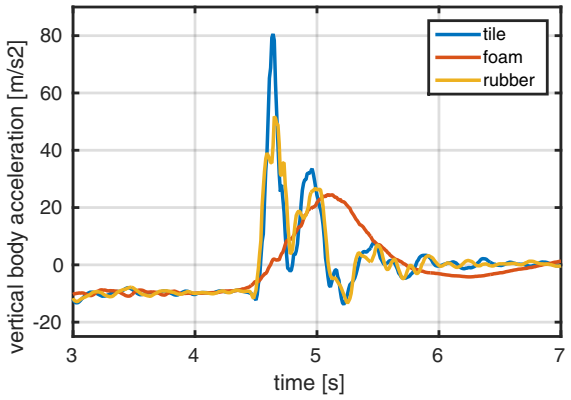

Fig. 5: Vertical acceleration of the SMC robot body while landing from a jump on three different ground surfaces. Note that the machine is in flight when the vertical acceleration is measured as approximately -9.81 m/s^2. The differences in dynamic response on the three surfaces is most dramatic at the moment of impact, at approximately 4.5 s. The hard tile results in the sharpest acceleration at impact, hard rubber shows less, and soft foam results in much slower impact dynamics. Each data plot consists of the average of ten trials and the results are repeatable enough to clearly distinguish the impact events: the standard deviation of the data at impact was less than a quarter of the peak average value.

TABLE II: Values of ground stiffness: in-situ measurement by the SMC robot and lab-bench measurement

Ground type	In-situ robot measurement, [kN/m]	Lab-bench measurement, [kN/m]
Foam pad	7.5	20
Rubber on Foam	11.1	50
Hard rubber	120	300

measured by an IMU at 800 Hz. Each data plot consists of the average of ten trials, though the measurements were very repeatable: the standard deviation measured at the impact event was less than a quarter of the peak measured value[5].

The results in Fig. 5 show the robot transitioning from flight, where the acceleration is measured as -9.81 m/s^2, to landing. The three surfaces—lab tile, rubber and foam—are clearly differentiated by the observed vertical acceleration of the body in the first 5-10 ms of landing: hard lab tile results in the largest impact acceleration at landing, followed by the rubber material, and then the soft foam. This result shows that the robot can differentiate surface types by observing its own response to impact events.

C. Measuring ground friction

Fig. 6 shows results of measuring the coefficient of friction of a ground surface in-situ. To perform this test, the robot stood still on the ground surface. Three legs were commanded stiff impedances to support the weight of the robot so that a fourth leg—the "free leg"— could be used to interact with the ground surface. The free leg applied a constant vertical force into the ground and then applied an increasing horizontal force. Horizontal force was increased until motion in the leg was sensed. The coefficient of friction was calculated from the ratio of horizontal to vertical force. Fig. 6 shows repeated trials on four ground surfaces: tile, plastic (polycarbonate), rubber flooring and foam core.

Table III compares friction measurements made with the SMC robot to values measured with lab-bench measurements. In the lab-bench measurement, the friction coefficient between the footpad material and the ground surface was measured by placing the ground surface at an increasing angle with respect to horizontal and observing when a mass began to slide on the surface. At this critical angle, the ratio of normal force and sliding force were used to calculate static friction. The results in Table III show that the friction coefficients measured by the robot were large compared to the lab-bench measurements, but that trends—i.e., rubber has higher friction than plastic—compared favorably. The consistently large values of ground friction measured by the SMC robot likely arise from a dead-band in the horizontal force when the leg is preloaded vertically and will be addressed in future tests.

V. Discussion & Future Work

The goal of this research is to increase the capability of robot legged locomotion over unexplored and variable terrain. The presented results show that changes in surface impedance has a large effect on locomotion behavior, and stability in particular. Behavior changes caused from variations in foot-ground impedance are hard to reliably predict a priori in simulation because they require accurate models

[5]The floor peak acceleration was 80 m/s^2 with a standard deviation of 19 m/s^2; rubber peak: 51, deviation 11; foam peak: 25, deviation 4.

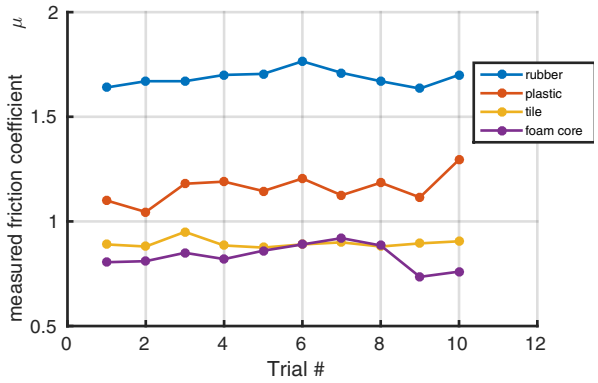

Fig. 6: The coefficient of static friction, as measured by the SMC robot in-situ. The test was performed by finding the ratio of horizontal to vertical force that causes a foot to slip on the surface. Each measurement can be made in approximately 3 seconds. Measurements on four surfaces were each repeated 10 times and the robot was physically moved between trials.

TABLE III: Values of static friction: in-situ measurement by the SMC robot and lab-bench measurement

Ground type	In-situ robot measurement	Lab-bench measurement
Rubber	1.7	1.4
Plastic	1.1	0.6
Foam core	0.8	0.5

of both the leg actuator and the interaction port between the foot and the terrain. Acquiring a complete model of the leg actuator may be costly, but should be theoretically possible. But, accurately predicting the interaction behavior of the foot and the ground must be aided by in-situ testing [39]: as with any mobile robot, the world the robot interacts with is infinitely variable and complex. For example, within 100 meters of the lab where the Super Mini Cheetah is kept, there are many surface types available: tile, foam, rug, concrete, wood, grass, dirt, gravel and sand. Most of these surfaces have time varying properties caused by weather and human activity.

Due to the challenge of modeling ground properties a priori, legged robots must become capable instruments for empirical observation of their environment and their own behavior. In this paper, we showed that a hopping gait can be self-disturbed in order to induce a repeatable disturbance response. Assessing broadly useful metrics of stability for legged robots is an important unsolved problem; stability predictions should answer the question "how likely is it that the desired locomotion behavior will work in the current setting?" Based on our experience with the SMC robot, we find the presented disturbance response data to correspond to a useful metric of stability: gaits with faster disturbance responses perform more reliably. It is encouraging that the disturbance-response experiment seems well suited for automation: reliable robot hardware could perform these tests without human intervention. In addition, the SMC robot

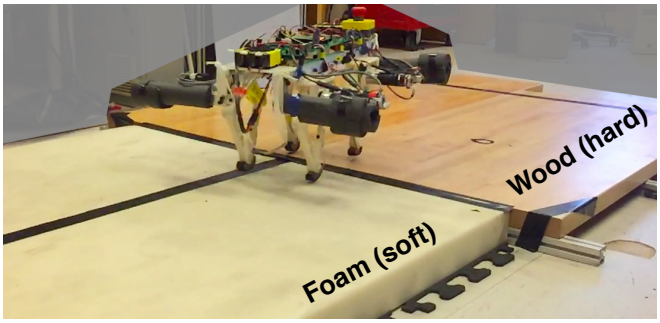

Fig. 7: An image of the SMC robot in mid-flight during running while transitioning from a hard wood surface to a soft foam surface. The preliminary experiments of this transition exhibit the need for real-time ground property measurement and controller adaptation. Please see the accompanying video attachment for video of this experiment.

is capable of perceiving that a fall has occurred and is often capable of standing up and restarting operation. The disturbance responses may also be interpreted online by the robot, as responses resemble systems with much lower system order—i.e., second order linear systems (see Fig. 2).

Controller development for dynamic robot locomotion remains an open research topic, and it is likely that further study will yield better performance than the controllers used in this study. The research community may benefit from searching for a single controller that always performs optimally, but our results present new evidence that relatively simple control systems can provide baseline performance to enable refinement through continued use and empirical observation. The hopping controllers presented in this study have been used as a basis for forward running and turning behaviors, which present a rich set of capabilities to use the robot to explore a wide range of environments. For instance, the SMC robot is capable of following high-level commands—e.g., "run forward ten steps", "turn left 45 degrees"—to navigate rooms and outdoor spaces. This, combined with the ability to measure ground properties should enable the robot to build spatial maps that include detailed terrain properties. Please see the accompanying video for examples of these behaviors.

In ongoing future work, we are studying forward running between hard and soft ground surfaces. For example, Fig. 7 shows the SMC robot in mid-flight while running from a hard wood to soft foam surface. These experiments do not yet include dynamic terrain measurement or controller switching. Initial results can be seen in the accompanying video: the robot can sometimes manage the transition from hard to soft ground, but without much of the typical grace of legged animals. Smoothly running over this type of ground transition will require both further controller development to find gaits that operate well in different terrain and during transition, as well as faster identification of ground properties.

VI. Conclusion

This paper presented experimental data of hopping over hard and soft ground with the MIT Super Mini Cheetah

robot. The hopping experiments measured 1.) the response of the robot to a self-disturbance which applied an additional force trajectory to disrupt normal hopping and 2.) the vertical accelerations of the body. the results showed that different controllers were better suited for different surfaces, and multiple trials showed that the disturbance response was repeatable. Given that ground impedance can effect locomotion behavior, methods to measure ground impedance and surface friction in-situ were developed. These two capabilities—measuring locomotion performance on different surfaces, and measuring surface properties in-situ—are important for increasing the skill of dynamic robot locomotion over unexplored, variable terrain. Finally, initial results of a more advanced locomotion task—running forward from hard to soft ground—were discussed to highlight future work in perception-driven controller selection of dynamic locomotion.

VII. Acknowledgments

The authors thank the DARPA Maximum Mobility and Manipulation (M3) Program, the MIT Undergraduate Research Opportunities Program (UROP) and the Louis G. Siegle Fellowship for supporting this work.

We also thank Debbie Ajilo, Michael Farid, Hans Susilo and Michael Chuah for contributions to the SMC robot.

References

[1] Bosworth W, Kim S, & Hogan N. "The MIT Super Mini Cheetah: A small, low-cost quadrupedal robot for dynamic locomotion." IEEE SSRR 2015.

[2] Park, H, Chuah M, and Kim S. "Quadruped Bounding Control with Variable Duty Cycle via Vertical Impulse Scaling." (IROS 2014).

[3] Massie, Thomas H., and J. Kenneth Salisbury. "The phantom haptic interface: A device for probing virtual objects." Proceedings of the ASME winter annual meeting, symposium on haptic interfaces for virtual environment and teleoperator systems. Vol. 55. No. 1. 1994.

[4] Saranli, Uluc, Martin Buehler, and Daniel E. Koditschek. "RHex: A simple and highly mobile hexapod robot." The International Journal of Robotics Research 20.7 (2001): 616-631.

[5] Kim, S., Clark J., and Cutkosky M. "iSprawl: Design and tuning for high-speed autonomous open-loop running." The International Journal of Robotics Research 25.9 (2006): 903-912.

[6] Sprowitz, Alexander, et al. "Towards dynamic trot gait locomotion: Design, control, and experiments with Cheetah-cub, a compliant quadruped robot." The International Journal of Robotics Research 32.8 (2013): 932-950.

[7] Semini, Claudio, et al. "Design of HyQa hydraulically and electrically actuated quadruped robot." Proceedings of the Institution of Mechanical Engineers, Part I: Journal of Systems and Control Engineering (2011): 0959651811402275.

[8] Hutter, Marco, et al. "StarlETH: A compliant quadrupedal robot for fast, efficient, and versatile locomotion." 15th International Conference on Climbing and Walking Robot-CLAWAR 2012. No. EPFL-CONF-181042. 2012.

[9] Sreenath, K., et al. "A compliant hybrid zero dynamics controller for stable, efficient and fast bipedal walking on MABEL." IJRR (2011).

[10] Grimes, Jesse A., and Jonathan W. Hurst. "The design of ATRIAS 1.0 a unique monoped, hopping robot." CLAWAR 2012.

[11] Pratt, Gill, and Matthew M. Williamson. "Series elastic actuators." Intelligent Robots and Systems 95.'Human Robot Interaction and Cooperative Robots', Proceedings. 1995 IEEE/RSJ International Conference on. Vol. 1. IEEE, 1995.

[12] Raibert, Marc H. Legged robots that balance. Vol. 3. Cambridge, MA: MIT press, 1986.

[13] Seok, Sangok, et al. "Actuator design for high force proprioceptive control in fast legged locomotion." Intelligent Robots and Systems (IROS), 2012 IEEE/RSJ International Conference on. IEEE, 2012.

[14] Krasny, Darren P., and David E. Orin. "Generating high-speed dynamic running gaits in a quadruped robot using an evolutionary search." Systems, Man, and Cybernetics, Part B: Cybernetics, IEEE Transactions on 34.4 (2004): 1685-1696.

[15] Coros, Stelian, et al. "Locomotion skills for simulated quadrupeds." ACM Transactions on Graphics (TOG) 30.4 (2011): 59.

[16] Dai, H., Valenzuela A., and Russ Tedrake. Whole-body motion planning with simple dynamics and full kinematics. MIT CSAIL, 2014.

[17] Wensing, P., and Orin D. "High-speed humanoid running through control with a 3D-SLIP model." Intelligent Robots and Systems (IROS), 2013.

[18] Lee, Sung-Hee, and Ambarish Goswami. "Reaction mass pendulum (RMP): An explicit model for centroidal angular momentum of humanoid robots." Robotics and Automation, 2007 IEEE International Conference on. IEEE, 2007.

[19] Pratt, Jerry, et al. "Virtual model control: An intuitive approach for bipedal locomotion." The International Journal of Robotics Research 20.2 (2001): 129-143.

[20] Semini, C, et al. "Design of HyQa hydraulically and electrically actuated quadruped robot." J of Sys & Cont Eng (2011).

[21] Hutter, Marco, et al. Quadrupedal locomotion using hierarchical operational space control. The International Journal of Robotics Research (2014): 0278364913519834

[22] Johnson, Amy M., and Daniel E. Koditschek. "Toward a vocabulary of legged leaping." Robotics and Automation (ICRA), 2013 IEEE International Conference on. IEEE, 2013.

[23] Hurst, Jonathan. (2015, April 27). "ATRIAS Bipedal Robot: Takes a Walk in the Park". Retrieved from https://www.youtube.com/watch?v=dl7KUUVHC-M, Sep 2015.

[24] Boston Dynamics. (2010 April 22). "BigDog Overview (Updated March 2010)". Retrieved from https://www.youtube.com/watch?v=cNZPRsrwumQ, Sep 2015.

[25] Boston Dynamics. (2015 Feb 9). "Introducing Spot". Retrieved from https://www.youtube.com/watch?v=M8YjvHYbZ9w, Sep 2015.

[26] Kim, Sangbae & MIT. (2014 Sep 15). "MIT Robotic Cheetah". Retrieved from https://www.youtube.com/watch?v=XMKQbqnXXhQ, Sep 2015.

[27] Murphy, Michael P., et al. "The littledog robot." The International Journal of Robotics Research (2010): 0278364910387457.

[28] "Darpa Robotics Challenge Finals 2015." DARPA. Accessed August 2015. "http://www.theroboticschallenge.org".

[29] Buchli, Jonas, et al. "Compliant quadruped locomotion over rough terrain." Intelligent Robots and Systems, 2009. IROS 2009. IEEE/RSJ International Conference on. IEEE, 2009.

[30] Ahn, Jooeun, and Neville Hogan. "Long-range correlations in stride intervals may emerge from non-chaotic walking dynamics." PloS one 8.9 (2013): e73239.

[31] Byl, Katie, and Russ Tedrake. "Metastable walking machines." The International Journal of Robotics Research 28.8 (2009): 1040-1064.

[32] Miller, Bruce, John Schmitt, and Jonathan E. Clark. "Quantifying disturbance rejection of SLIP-like running systems." The International Journal of Robotics Research (2012): 0278364912439613.

[33] Krotkov, Eric. "Active perception for legged locomotion: every step is an experiment." International Symposium on Intelligent Control. IEEE, 1990.

[34] Hopflinger, Mark, et al. "Haptic terrain classification for legged robots." IEEE International Conference on Robotics and Automation (ICRA), 2010.

[35] Walas, Krzysztof. "Terrain Classification and Negotiation with a Walking Robot." Journal of Intelligent & Robotic Systems 78.3-4 (2015): 401-423

[36] Ordonez, Camilo, et al. "Terrain identification for RHex-type robots." SPIE Defense, Security, and Sensing. International Society for Optics and Photonics, 2013.

[37] Garcia Bermudez, Fernando L., et al. Performance analysis and terrain classification for a legged robot over rough terrain. IEEE/RSJ International Conference on Intelligent Robots and Systems, 2012.

[38] Chuah, Meng Yee, and Sangbae Kim. "Enabling force sensing during ground locomotion: A bio-inspired, multi-axis, composite force sensor using discrete pressure mapping." Sensors Journal, IEEE 14.5 (2014): 1693-1703.

[39] Hogan, Neville. "A General Actuator Model Based on Nonlinear Equivalent Networks." Mechatronics, IEEE/ASME Transactions on 19.6 (2014): 1929-1939.